

Synthesis of mesoporous silicon directly from silicalite-1 single crystals and its response to thermal diffusion of ZnO clusters

Jiang Zhu · Ruibin Liu · Jun Xu · Changgong Meng

Received: 4 November 2010 / Accepted: 17 January 2011 / Published online: 29 January 2011
© Springer Science+Business Media, LLC 2011

Abstract This article describes the preparation of mesoporous silicon granules with a layered structure directly from silicalite-1 single crystals. The silicalite-1 single crystals were thermally reduced in vacuum at 630 °C, with the original shape retained. The samples are confirmed as crystalline silicon by X-ray diffraction and transmission electron microscope. The silicon granule is composed of a monocrystalline surface and polycrystalline layered interior. A surface area of around $66 \text{ m}^2 \text{ g}^{-1}$ and the pore size centered at 3.7 nm were obtained from nitrogen porosimetry, BET and BJH analysis. The ZnO clusters have been loaded into the porous silicon granule by thermal diffusion method. The photoluminescence emission centered at 3.44 eV originates from the small particles of ZnO and the band at 2.81 eV may be due to both an oxidized surface and quantum confinement effects. The microstructure in this silicon granule is very different from those in etched samples. The synthetic design demonstrates an interesting way from the microporous zeolite to mesoporous silicon and enlarges the structural diversity of porous silicon crystal.

Abbreviations

XRD	X-ray powder diffraction
SEM	Scanning electron microscope
TEM	Transmission electron microscope

Electronic supplementary material The online version of this article (doi:[10.1007/s10853-011-5300-7](https://doi.org/10.1007/s10853-011-5300-7)) contains supplementary material, which is available to authorized users.

J. Zhu · R. Liu · J. Xu · C. Meng (✉)
Department of Chemistry, Dalian University of Technology,
116023 Dalian, China
e-mail: cgmeng@dlut.edu.cn

HRTEM	High resolution TEM
SAED	Selected area electron diffraction
EDS	Energy dispersion spectrometer
PL	Photoluminescence
BET	Brunauer-Emmet-Teller
BJH	Barret Joyner Halendar

Introduction

Porous silicon was first reported in 1956 and it was in the year of 1990 that the photoluminescence from porous silicon was discovered in ambient, which evoked people's passion to develop its new applications based on its unique optical property [1]. In recent years, porous silicon has been found of many excited applications, especially in sensors, manufacture, energy, and bio-medicine [2–6]. Porous silicon was usually synthesized from silicon wafers via chemical etching method. The structure of porous silicon is determined by the doping of the substrate and etching conditions [7]. However, the similar structure with the pore growing along the $\langle 100 \rangle$ direct deters the abundance of porous silicon structures, due to the similar etching circumstances [8]. Considerable attentions have been paid to synthesize porous silicon by displacement reaction which has been used in the synthesis of crystal silicon for decades [9, 10]. In 2003 silicon with column structure was achieved by the electrochemical process from solid oxide in molten calcium chloride electrolyte at 850 °C, using a molybdenum or tungsten wire as the electrode [11, 12]. Natural specimens of SiO_2 , such as microshells of diatoms and Mediterranean sands, were successfully converted to silicon replicas by heat reduction reactions [13, 14]. In this article the authors demonstrate how to convert the silicalite-1

single crystals (MFI type), a special form of SiO_2 with ordered pore and channels, into mesoporous silicon by magnesiothermic reduction reaction, during which the original shape and fine features were well preserved. The structure is very different from those by traditional etching method. ZnO has been impregnated into the as-synthesized sample by a thermal diffusion method and the changes in photoluminescence spectra were discussed. The results will allow us to discuss the origin and the characteristics of this material systematically by studying the process from porous zeolites to porous silicon.

Experimental

Preparation

Here silicalite-1 single crystal was synthesized by a typical hydrothermal method. The composition of the gel is as following: molar ratio $6.2 \text{ Na}_4\text{EDTA}:1.5\text{TPABr}:20\text{SiO}_2:1.2\text{sucrose}:888\text{H}_2\text{O}$. After reaction at 170°C for 10 days, the product was filtered and washed with water and ethanol for several times until the pH value of the solution is about 7. The as-synthesized single crystals were dried at 100°C for 2 h and then calcined at 550°C for 5 h in air.

The reduction reaction is described as following: a mixture of magnesium powder and silicalite-1 single crystals (0.6 g, molar ratio $\text{Mg}:\text{SiO}_2 = 2.5:1$) was placed in a ceramic boat in a tube furnace. After the furnace was vacuumized, the mixture was heated to a temperature of 630°C and maintained for 2 h. The products were collected and immersed in HCl solution (with molar ratio of $\text{HCl}:\text{H}_2\text{O}:\text{EtOH} = 0.50:3.57:6.73$) for 6 h at room temperature to selectively remove the MgO and excessive Mg powder. The sample was then exposed to a HF solution (with molar ratio of $\text{HF}:\text{H}_2\text{O}:\text{EtOH} = 0.70:0.74:5.92$) for 10 min to ensure that any oxide unreacted or formed during the HCl treatment was eliminated completely. At last the obtained silicon granules were dried at 100°C for 4 h.

ZnO was impregnated into porous silicon by two steps. Porous silicon granules (0.5 g) and Zn powder (2 g) were placed at the opposite ends of a glass tube that was sealed. The reactor was heated at 700°C with a heating rate of less than $1^\circ\text{C}/\text{min}$ and maintained for 20 h. After the reactor was cooled down to room temperature, the sample was transferred into a crucible and calcined in air at 550°C to get all the zinc species into oxides.

Characterizations

The X-ray powder diffraction (XRD) analysis was taken to verify the sample structure using a Shimadzu XRD-6000 diffractometer with $\text{Cu K}\alpha$ radiation ($\lambda = 1.54060 \text{ \AA}$),

operating at a voltage of 40 kV and a current of 30 mA. The morphologies were observed by a JSM-5600LV scanning electron microscope (SEM) operated at 5.0 kV. Transmission electron microscope (TEM) and high resolution TEM (HRTEM) images were obtained with a Philips Tecnai G² 20 instrument, which was equipped with selected area electron diffraction (SAED) and operated with an accelerating voltage of 200 kV. The energy dispersive spectrometry (EDS) was conducted by an INCA energy dispersive spectrometer installed on the TEM. The silicon granules were broken into pieces by ultrasonication to ensure that the pieces of granules were thin enough for the TEM measurement. The N_2 adsorption-desorption isotherm was obtained by using a Micrometrics ASAP-2020 analyzer. The photoluminescence (PL) emission spectrum was measured with a Fluorescence spectrometer (Perkin Elmer LS55) using a xenon lamp as the excitation source.

Results and discussion

The average yield of the reduction reaction is about 90%. If the molar ratio of $\text{Mg}:\text{SiO}_2$ is less than 2:1, the average yield decreases to no more than 80%; when the molar ratio of $\text{Mg}:\text{SiO}_2$ increases to more than 3:1, Mg_2Si begins to be found in the products. If the reaction temperature is lower than 600°C , the reaction does not take place; if the temperature is higher than 700°C , some granules begin to crack on the surface or even split into pieces (Fig. S1 in supplementary information).

To verify the success of the reaction, the products were examined by XRD analysis. Figure 1a is the XRD pattern of the silicalite-1 single crystals. The XRD pattern displayed in Fig. 1b revealed that the observed diffraction peaks are, respectively, indexed to (111), (220), (311), (400), and (331) planes of cubic crystal silicon (JCPDS card no. 27-1402), which indicate the residual impurities were efficiently removed.

The SEM image of silicalite-1 single crystals is shown in Fig. 2a. Every silicalite-1 single crystal granules possesses a regular shape and reaches about $150 \mu\text{m}$ along c axis. As revealed in Fig. 2b, the shape of silicon granule was well retained and there is no measurable change in the size. The modest temperature and appropriate reaction time prevented the granules from coarsening and shrinking. In addition the formation of a continuous refractory magnesia phase, intertwining with the silicon, supported the framework in a certain extent. Thus, the original shape of the granule could be preserved after MgO dissolution in acid treatments [13].

To confirm the crystalline phase and composition, TEM was conducted on the cross sections of some silicon granules and the authors have found two kinds of structures

Fig. 1 XRD patterns of silicalite-1 single crystals (a) and the as-synthesized porous silicon granules (b)

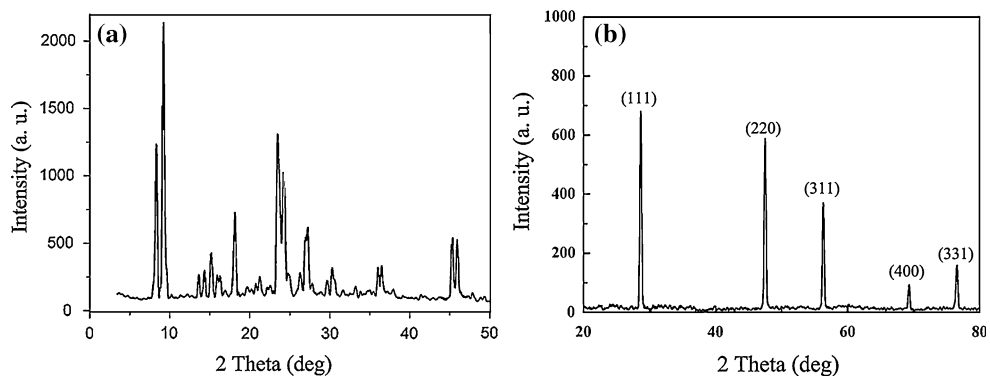
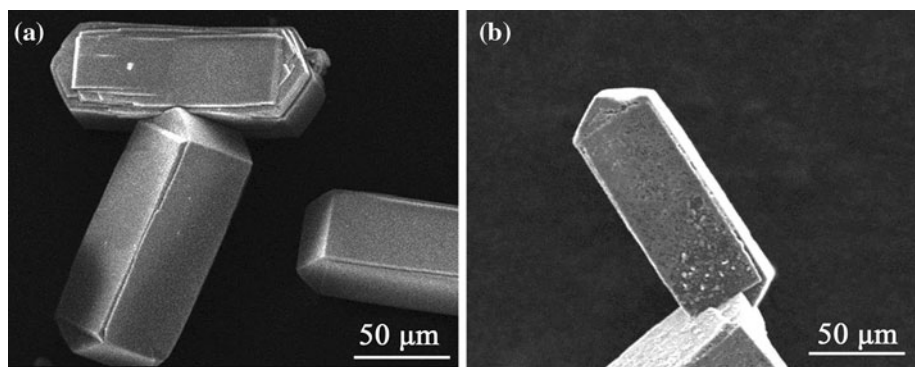


Fig. 2 SEM images of silicalite-1 single crystals (a) and the as-synthesized porous silicon granules (b)



in the sample: lamellar pieces and layers with pores. Figure 3a revealed a TEM image of a lamellar piece. The uniform and homogeneous contrast reflects its uniform thickness. From the TEM image of a cross section (Fig. 3b), the authors can see that this piece is actually composed of thinner pieces. The HRTEM image in Fig. 3c demonstrates the clear and uniform lattice fringes. The lattice spacing is calculated to be 0.32 nm, which is consistent with the spacing between the (111) planes in a face-centered cubic crystal silicon. The sharply diffraction spots shown in the SAED pattern in the inset are similar to the pattern of single crystal silicon taken along the [100] zone axis. Both the HRTEM and SAED analysis suggest the monocrystalline morphology in this area [15]. Figure 3d is the TEM image of the layered structure and there were numerous and irregular pores with approximate 200 nm in diameter on each layer. Individual pores were not clearly imaged, mainly due to the overlapping of adjacent layers. Figures 3e shows an amplified TEM image of several overlapping thin layers. A single intact pore with about 100 nm in diameter on the top thin layer is clearly revealed. The layers also exhibit uniform and homogeneous contrast, reflecting their uniform thickness. Further study has been carried out with the HRTEM analysis shown in Fig. 3f. This structure was agglomerated by small silicon crystallites with approximately 5 nm in diameter, presented by the uniform lattice fringes with different orientations [10].

The lattice space is also consistent with the spacing between the (111) planes in crystal silicon. Indexed in the SAED pattern in the inset are well defined diffraction rings. Both the HRTEM and SAED analysis obviously exhibit that this layered structure is polycrystal [15].

In order to determine the real composition of the sample EDS was used and the data is shown in Fig. 4. There are several signals for C, O, Cu, and Si. The occurrence of the Cu and the C peak is due to the Cu grid and the C film coating on the Cu grid. Compared with the Si peaks, the intensity of O peak is very low, which may originate from a small amount of oxidized sample. The EDS microanalysis of oxygen is not accurate, thus the authors could only conclude that there exists a small amount of oxygen in the silicon granules, owing to exposure to air during drying [16].

The N₂ adsorption–desorption isotherm for the sample was obtained at –196 °C and shown in Fig. 5a. The isotherm can be classified as a type IV isotherm according to the IUPAC nomenclature. The abrupt change occurs in the relative pressure range of 0.9–1.0, which also reveals a relatively large pore and layered structure [17]. The b type hysteresis loop appears at p/p⁰ of 0.4–1.0 and the two branches are nearly parallel over a wide range, indicating the presence of narrow slit-like pores [18]. The sample exhibits an N₂ Brunauer-Emmet-Teller (BET) surface area of 22.18 m² g⁻¹. Shown in Fig. 5b, the Barret-Joyner-Halendar (BJH) pore distribution centered at 3.7 nm.

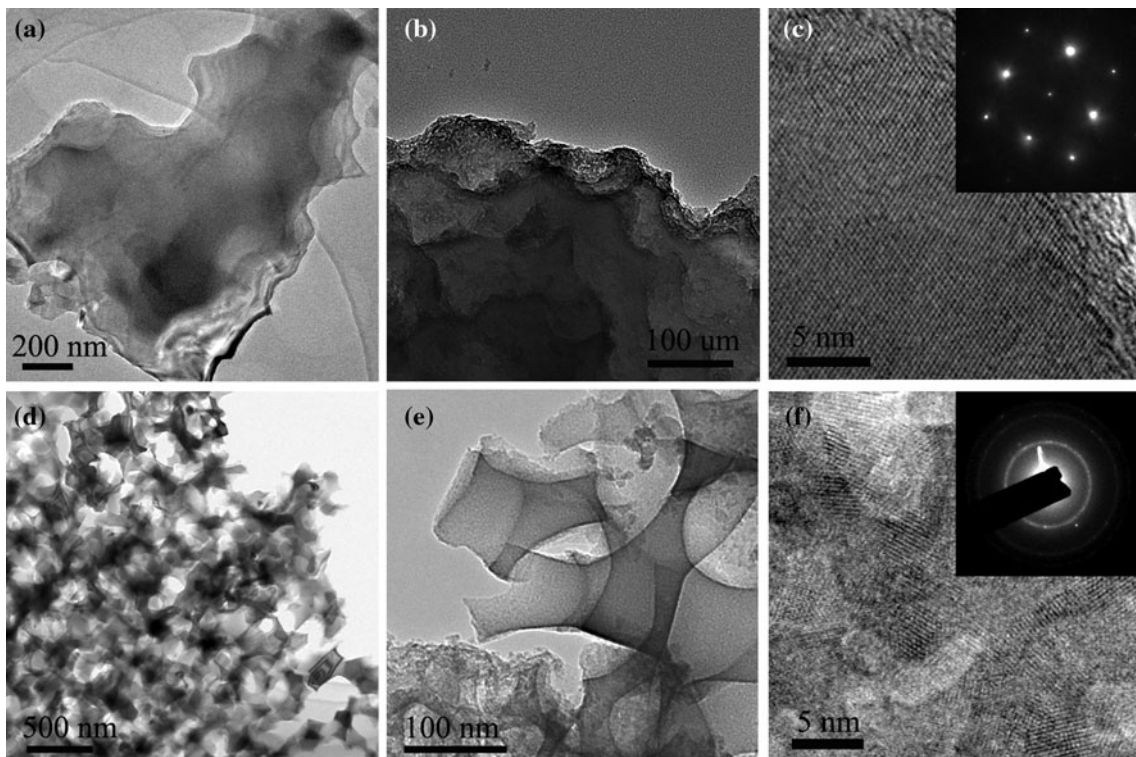


Fig. 3 TEM image (a), amplified TEM iamage (b), and HRTEM image (c) of a monocrystal piece, TEM image (d), amplified TEM iamage (e), and HRTEM image (f) of several overlapping thin layers

structure. TEM image (d) and HRTEM image (e) of a monocrystal piece, in the insets of (c), and (f) are the corresponding SAED patterns

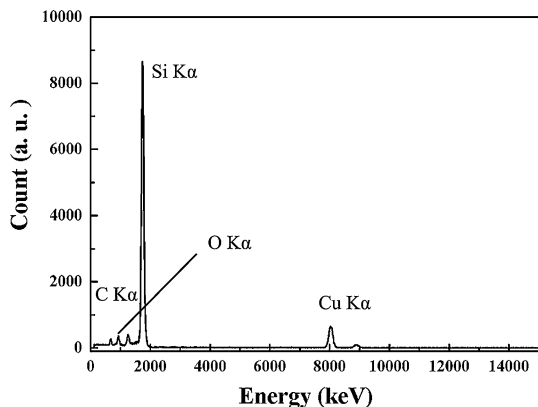


Fig. 4 The full scaled EDS results of a region on a silicon granule observed in TEM

From the above results it seems to obtain such a conclusion that the monocrystalline pieces come from the surface of the silicalite-1 single crystals and the layered structure comes from the interior. When heated in vacuum, Mg gas could rapidly enwrap the silicalite-1 granule and the homogeneous surface is reduced to monocrystal directly and rapidly. Owing to some differences between the surface and the inside, hollow locations occur on the interface [19]. Mg gas enters the insider along these locations and begins to reduce the interior. At the neighbor

regions Si–O–Si was reduced to Si–Si bond and the Si–Si bonds grew to chain and nets along the original channels and pores in the zeolite. The produced silicon intertwined with the formation of continuous magnesia phase. Thus, the narrow mesoporosity of 3.7 nm formed when the refractory magnesia phase was dissolved in HCl and HF solutions. However, the authors have to admit that this is the only speculation and the further related study is currently under way (Fig. 6).

The PL emission spectra of the sample before and after ZnO loaded were obtained at room temperature and presented in Fig. 4a, b ,respectively. Before ZnO loaded, the broad band in blue region centered at 622 nm is quite intense, with an excitation at 450 nm. After ZnO loaded, the band of 622 nm for porous silicon does not emerge. The band around 360 nm suggests that ZnO is formed in the pores of porous silicon. Generally, the PL emission band of bulk ZnO occurs at 370 nm. The blue shift is attributed to small particle size effect from the small particles encapsulated in the pores [20]. Also, the infiltration of ZnO affects the emission center of the PL band to some extent, which turns a blue shift as the ZnO content increasing [21]. The blue emission at 442 nm was originally interpreted by the direct interband radiative recombination process. The surface oxidation during the heat

Fig. 5 Nitrogen adsorption–desorption isotherm of the porous silicon granules (a) and the BJH pore size distribution (b)

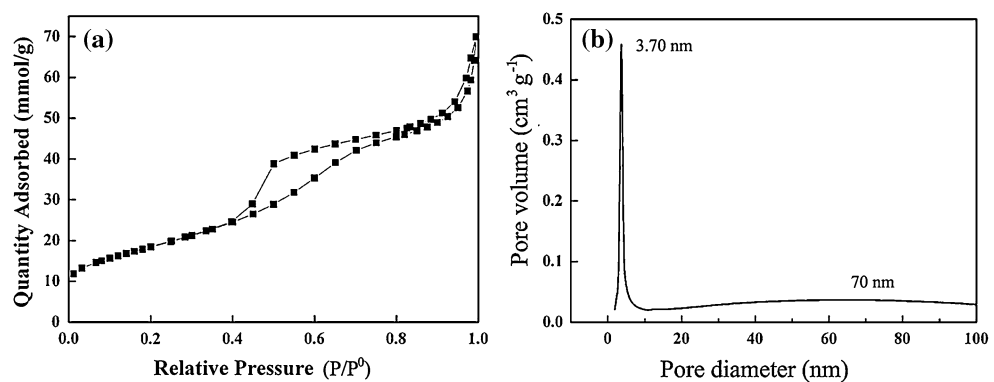
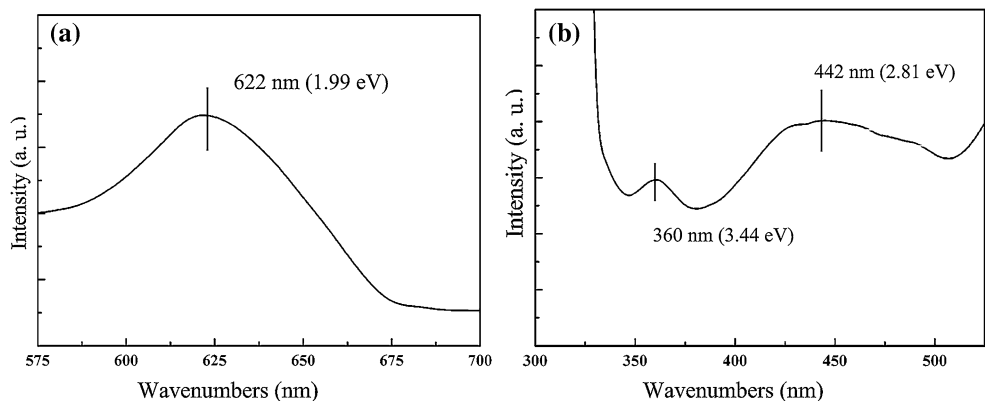


Fig. 6 Photoluminescence spectra of synthesized porous silicon before (a) and after (b) ZnO loaded



treatment decreases the size of silicon nanocrystals and the blue shifted energy level was involved due to the quantum confinement effect [22]. Moreover, after the ZnO loaded the stable defect in transition metal oxides generally gives too deep impurity levels, which might also influence the light emission of porous silicon [23].

Conclusions

In general, mesoporous crystal silicon has been synthesized from silicalite-1 single crystal by a thermal reduction reaction. Two structures including monocrystalline piece and polycrystalline layer have been found in the retained shape. The possible mechanism for the formation of porous structure has been discussed. ZnO has been loaded in the porous silicon by a thermal diffusion method and the changes in the PL spectra are considered to originate from small particle size effect. This general approach has considerable promise for the further extensive study of the new structures of porous silicon.

Acknowledgements The authors are grateful to Experimental Center of Chemistry, Dalian University of Technology (China) for providing the necessities in experiments. Many thanks are dedicated to Mr. Jian Wu for his continuous help.

References

1. Canham LT (1990) *Appl Phys Lett* 57(10):1046
2. Zhao Y, Li D, Sang W, Yang D, Jiang M (2007) *J Mater Sci* 42:8496. doi:[10.1007/s10853-007-1749-9](https://doi.org/10.1007/s10853-007-1749-9)
3. du Plessis M (2007) *Sensor Actuat a-Phys* 135(2):666
4. Bhattacharya E, Rani HA, Babu UV, Rao PRS, Bhat KN, Martin J (2005) *Phys Status Solidi A* 202(8):1482
5. Torres-Costa V, Martin-Palma RJ (2010) *J Mater Sci* 45:2823. doi:[10.1007/s10853-010-4251-8](https://doi.org/10.1007/s10853-010-4251-8)
6. Park JH, Gu L, von Maltzahn G, Ruoslahti E, Bhatia SN, Sailor MJ (2009) *Nat Mater* 8(4):331
7. Ohmukai M, Okada K, Tsutsumi Y (2005) *J Mater Sci Mater Electron* 16:119
8. Chuang SF, Collins SD, Smith RL (1989) *Appl Phys Lett* 55(7):675
9. Breslin MC, Ringnalda J, Xu L, Fuller M, Seeger J, Daehn GS, Otani T, Fraser HL (1995) *Mater Sci Eng A* 195:113
10. Biehl E, Schubert U, Kubel F (2001) *New J Chem* 25:994
11. Nohira T, Yasuda K, Ito Y (2003) *Nat Mater* 2:397
12. Jin X, Gao P, Wang D, Hu X, Chen G (2004) *Angew Chem Int Ed* 43:733
13. Bao Z, Weatherspoon MR, Shian S, Cai Y, Graham PD, Allan SM, Ahmad G, Dickerson MB, Church BC, Kang Z, Abernathy HW III, Summers CJ, Liu M, Sandhage KH (2007) *Nature* 446:172
14. Hai NH, Grigoriantis I, Gedanken A (2009) *J Phys Chem C* 113:10521
15. Liu S, Kobayashi M, Sato S, Kimura K (2005) *Chem Commun* 37:4690
16. Richman EK, Kang CB, Brezesinski T, Tolbert SH (2008) *Nano Lett* 8:3075

17. Huo Q, Zhao D, Feng J, Weston K, Buratto SK, Stucky GD, Schacht S, Schüth F (1997) *Adv Mater* 9:974
18. Hilonga A, Kim J, Sarawade PB (2010) *J Mater Sci* 45:1264. doi: [10.1007/s10853-009-4077-4](https://doi.org/10.1007/s10853-009-4077-4)
19. Baldwin RK, Pettigrew KA, Ratai E, Augustine MP, Kauzlarich SM (2002) *Chem Commun* 17:1822
20. Singh RG, Singh F, Kanjilal D, Agarwal V, Mehra RM (2009) *J Phys D Appl Phys* 42(6):062002
21. Murugan AV, Heng OY, Ravi V, Viswanath AK, Saaminathan V (2006) *J Mater Sci* 41(5):1459. doi: [10.1007/s10853-006-7461-3](https://doi.org/10.1007/s10853-006-7461-3)
22. Li XX, Tang YH, Lin LW, Li JL (2008) *Microporous Mesoporous Mater* 111:591
23. Henrich VE, Cox PA (1994) *The Surface Science of Metal Oxides*. Cambridge University, Cambridge